



## Lipoprotein Oxidation and its Significance for Atherosclerosis: a Mathematical Approach

C. A. COBBOLD\*, J. A. SHERRATT AND S. R. J. MAXWELL<sup>†</sup>

Centre for Theoretical Modelling in Medicine,  
Department of Mathematics, Heriot-Watt University,  
Edinburgh EH14 4AS,  
U.K.

*E-mail:* C.A.Cobbold@ma.hw.ac.uk; jas@ma.hw.ac.uk

Atherosclerosis is a chronic disease which involves the build up of cholesterol and fatty deposits within the arterial wall. This results in the narrowing of the vessel lumen, which eventually restricts blood flow to vital organs such as the heart and lungs. These events may culminate in a heart attack or stroke, the commonest causes of death in the U.K. population. In this paper we study the early stages of atherosclerosis which include the build up of cholesterol within subendothelial cells to form what is known as a fatty streak, the earliest identifiable evidence of atherosclerosis. The deposition of cholesterol is believed to be a consequence of oxidation of circulating cholesterol-rich lipoproteins, in particular low density lipoproteins (LDLs). Via a mathematical model we investigate this process of oxidation within the context of an *in vitro* framework. We first recreate existing experimental results and then extend the model to investigate phenomenon not studied by current experimental protocols. We find that the model displays hysteresis which reveals some interesting insights into possible *in vivo* events. Mathematical analysis of this behaviour predicts that vitamin E supplementation is not as beneficial as high density lipoproteins (HDLs) and vitamin C. Furthermore, the scavenging of oxidants by HDL can provide an important first line of defence against LDL oxidation.

© 2002 Society for Mathematical Biology

### 1. INTRODUCTION

Atherosclerosis involves the build up of cholesterol and other fatty deposits within the arterial wall leading to the narrowing of the blood vessel lumen [see Fig. 1]. This has the consequence of restricting blood flow to vital organs which can eventually lead to various clinical syndromes such as heart attacks and strokes. These events are the leading causes of death in the developed world (Bowry and Ingold, 1999).

<sup>†</sup>Also at: Clinical Pharmacology, University of Edinburgh, Western General Hospital, Edinburgh EH4 2LH, U.K. *E-mail:* s.maxwell@ed.ac.uk

\*Author to whom correspondence should be addressed.

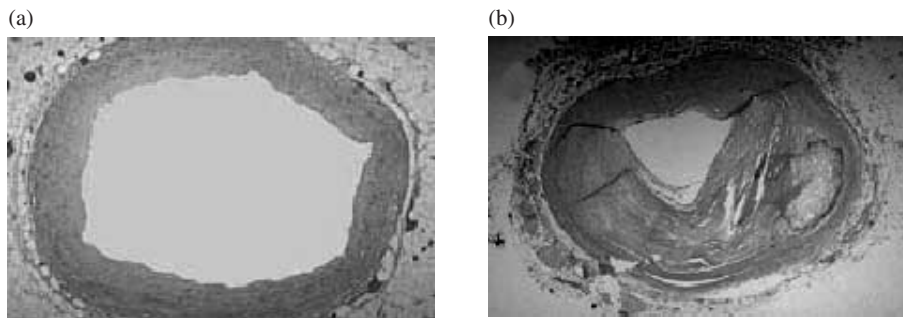


Figure 1. (a) Cross section of a normal artery lumen. The endothelial cells neighbour the lumen and no intimal thickening is present. (b) Severe atherosclerosis. On the right a calcified plaque has formed pushing against the endothelial cells forcing them to bulge into the lumen restricting blood flow.

The early events leading to atherosclerosis occur in the space between the endothelial cells and the smooth muscle cells (Fig. 2), a region of the blood vessel known as the subendothelium or intima. The process leading to the cholesterol deposits begins with the formation of fatty streaks. Accumulation of cholesterol within cells leads to the formation of 'foam cells' which reside in this intimal region of the vessel wall and constitute the fatty streak. At this stage no symptoms will be observed and in fact symptoms of atherosclerosis often do not reveal themselves until complications such as angina and coronary artery disease arise. The fatty streaks are often present in childhood and may not always progress to form the plaques which can be found in affected adults. [For a review see, Davies and Woolf (1990), and Esterbauer *et al.* (1992)]. The disease may remain asymptomatic for many years. However, critical restriction of blood flow or thrombosis leading to total occlusion of the vessel may lead to cardiovascular events such as heart attack or stroke later in life.

Normal arteries can cope with some blood vessel narrowing, as they are naturally larger than they need to be to achieve normal flow. Moreover, new blood vessels can often form to divert blood around problem areas. However, if the lipid accumulation progresses, atheromas or fibrous plaques will form, these have increased numbers of proliferating smooth muscle cells and extracellular lipid. This can erode the blood vessel wall and interfere further with blood flow and stimulate further plaque formation. Characteristic of the advanced stages of lesions, this generally appears in adulthood and progresses with time, and it is this stage at which complications may begin to arise.

**1.1. Early stages of atherosclerosis.** We are primarily interested in the early stages of atherosclerosis. Specifically we are focusing on the events which lead to the formation of the foam cells which constitute the fatty streak. In the initial stages of the disease foam cells are derived from macrophages, which internalize cholesterol and lipid as part of their normal function. However when large amounts

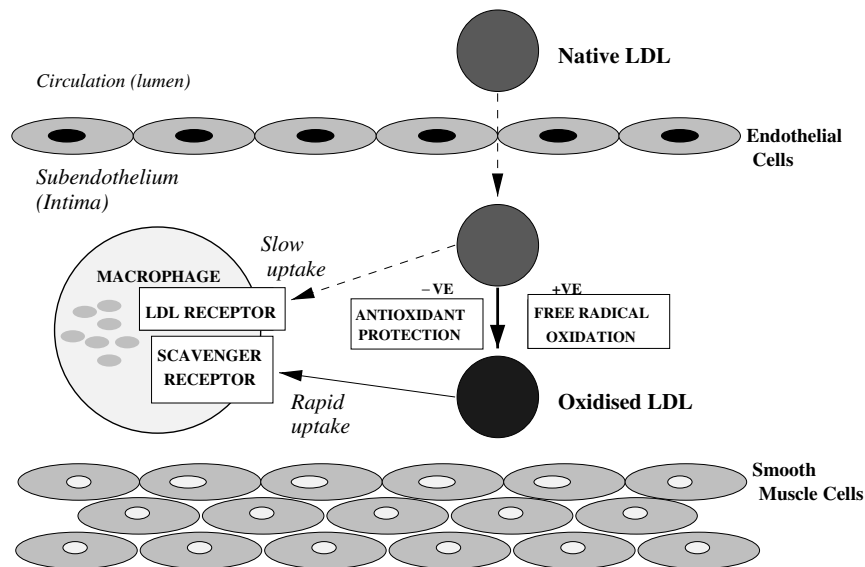


Figure 2. Schematic cross section of a blood vessel. The native LDL crosses the endothelium where it can then undergo oxidation via radical attack. Antioxidants in the intima and within the LDL particle are able to prevent this oxidation. However once oxidation has occurred the oxidized lipoprotein can be more rapidly taken up by cells. When a cell becomes overwhelmed with lipid it becomes a foam cell, a principal component of the early stages of atherosclerosis.

are ingested the cells can develop into the cholesterol laden foam cells. These cells are overwhelmed by the lipid and cannot reenter the lumen (Hamilton, 1997).

The cholesterol has been found to originate primarily from circulating plasma lipoproteins (Parthasarathy *et al.*, 1990; Stocker, 1999), specifically low density lipoproteins (LDLs). Native lipoprotein does not avidly accumulate in macrophages due to a negative feedback mechanism which down-regulates the expression of the lipoprotein receptor (Keaney *et al.*, 1999) on the cell surface. However, rapid progress in the understanding of cholesterol uptake occurred when Goldstein and coworkers (1977) discovered that macrophages possess a high up-take receptor, the scavenger receptor, which has an affinity for a modified form of the LDL. This modified form is now widely believed to be oxidized LDL (ox-LDL). Moreover, recent work has now provided evidence that ox-LDL exists *in vivo* (Steinberg *et al.*, 1989; Cox and Cohen, 1996). The main focus of this work is the process leading to oxidative modification of LDL in the subendothelial space.

**1.2. Lipoproteins.** The major carriers of cholesterol and other lipids through the body are lipoproteins. These particles are formed in the liver and gut from where they are then transported, via the blood plasma, to cells and tissue to provide lipid for use in cellular metabolism. The two lipoprotein subfractions responsible for cholesterol transport are LDLs and high density lipoproteins (HDLs) (Nielsen, 1999). LDL particles consist of a lipid core, a surface protein and antioxidant defences such as ubiquinol-10 and  $\alpha$ -tocopherol (vitamin E) (Bowry and Stocker,

1993; Francis, 2000). HDL is a smaller denser particle, but its structure is essentially the same. Both lipoprotein types are able to pass through the blood vessel wall into the intima. Oxidation is very unlikely in the plasma due to low radical flux and an increased antioxidant content. However, during lipoprotein residence in the less protective environment of the intima they are vulnerable to oxidation. This occurs via free radicals such as peroxy radicals which are released from cells and chemical reactions. They attack the lipoproteins, and once the particle's antioxidant defence is depleted, they initiate peroxidation of the lipid core. In the later stages of this process the surface protein also becomes modified, enabling the oxidized lipoprotein to be now recognized by the scavenger receptor (Cox and Cohen, 1996).

Although both LDL and HDL can undergo oxidation, only ox-LDL is recognized by the scavenger receptor (Parthasarathy *et al.*, 1990). This is probably due to differences in the surface protein of the two molecules (Cox and Cohen, 1996; Upston *et al.*, 1999). The fact that only modified LDL can be internalized by macrophages, helps to account for some of the proatherogenic effects associated with high plasma concentrations of LDL (Bjornheden *et al.*, 1996). However, it is the protective nature of high levels of HDL which is of particular interest here. Epidemiological data has revealed a strong inverse relationship between the risk of coronary artery disease and plasma HDL levels (Bonnetfont-Rousselot *et al.*, 1999).

Reverse cholesterol transport has been suggested as a mechanism whereby HDL can offer protection against atherosclerosis. This mechanism involves the transfer of cholesterol from both LDL and cells to HDL particles where they then return to the liver where the lipid is removed from the system (Tall, 1990). Although this has been a popular explanation, there is only limited evidence to support this theory. For example oxidized HDL has been shown to have a diminished capacity to accept cholesterol from cells (Francis, 2000). Moreover, genetic deficiency of LCAT, the enzyme facilitating reverse cholesterol transport, did not result in a marked increase in atherosclerosis (Tall, 1990). Consequently an alternative explanation has been proposed, whereby HDL particles provide protection against lipoprotein oxidation by directly interfering with the process, effectively acting as sponge for free radical attack. This may explain why HDL is the major carrier of peroxides in circulating plasma and account for the high percentage of oxidized HDL often found in the intimal region. We aim to investigate the hypothesis that HDL is a sacrificial target for oxidation by using a mathematical model to consider whether this mechanism can account for the level of protection revealed by epidemiological studies.

**1.3. LDL and HDL and antioxidant protection.** In order to investigate this potential protective mechanism we first discuss some of the details of HDL and LDL composition. Lipoproteins possess their own antioxidant defence against free radical attack. Vitamin E ( $\alpha$ -tocopherol) is a key component of this defence, with numerous *in vitro* experiments demonstrating that the onset of lipid peroxidation coincides with vitamin E depletion (Esterbauer *et al.*, 1992). On average an LDL

particle contains about six vitamin E molecules (Stocker, 1999) although depending on diet, this can vary from anything from 3 to 15 (Esterbauer *et al.*, 1992). Although the ratio of  $\alpha$ -tocopherol to lipid is actually the same for both lipoprotein types (Bowry *et al.*, 1992), the small size of HDL means that only 40% of HDL particles possess a vitamin E, the remainder having none.

When a free radical hits a lipoprotein it will preferentially react with a vitamin E molecule within the particle, as they are approximately 5 orders of magnitude more reactive than the components of the lipid core (Upston *et al.*, 1999). The resulting oxidized vitamin E, or  $\alpha$ -tocopherol radical, can be reduced back to a vitamin E molecule by ascorbate (vitamin C) molecules present in the aqueous environment of the intima (Niki *et al.*, 1984; Watanabe *et al.*, 1999). Ascorbate donates an electron, thus synergistically prolonging the protection provided by vitamin E (Doba *et al.*, 1985).

However, when a lipoprotein has had all its vitamin E molecules oxidized the lipid moiety becomes susceptible to lipid peroxidation. When sufficiently oxidized, not only can LDL particles be taken up by macrophages, they are also no longer able to leave the intima, unlike their unoxidized counterparts. This is in contrast to oxidized HDL particles which are not taken up by the scavenger receptor (Bowry *et al.*, 1992) and can still move freely out of the intima to return to the liver (Tall, 1998). It is these properties which may allow HDL to be effective sponges for radical attack; in addition there is a six fold higher concentration of HDL in plasma in comparison to LDL. By incorporating these key biological mechanisms and features into a mathematical model we will be able to examine the extent of protection afforded by HDL. Furthermore we can study the importance of antioxidants within the system.

**1.4. Experimental and mathematical models.** To date typical clinical and laboratory work concerning atherosclerosis and more specifically lipoprotein oxidation has been concerned with *in vitro* studies in which lipoproteins are exposed to radical generators, or epidemiological studies in which patients in various disease states are supplemented with antioxidants. *In vivo* work has largely focussed on animal models such as rabbits, which exhibit atherosclerosis on a significantly shorter timescale than humans. Experimental constraints leave intimal concentrations of most components of the lipoprotein system difficult to measure. In particular, the high reaction rate and the extensive range of targets has made radical production rates and biochemical events difficult to characterise and quantify. Despite these problems there have been significant advances in the understanding of atherosclerosis, but many questions remain.

Previous mathematical approaches to studying the processes involved in atherosclerosis have come in the form of fluid dynamics models where the effects of arterial thickening on blood flow have been considered (Hazel and Pedley, 1998). Movement of cholesterol through the blood vessel wall has also been studied, this was carried out using convection–diffusion equations (Saidel *et al.*, 1987; Neumann

*et al.*, 1990). A more recent series of articles by Stanbro (2000a,b,c) considered LDL oxidation by a specific radical, namely peroxyxynitrite, and studied these events on the scale of one LDL particle. In this paper we take a quite different approach motivated by questions concerning the protection offered by HDL. We incorporate features absent from *in vitro* experimental models but present *in vivo* and explicitly study the process of oxidation on the macro scale of the blood vessel intima. This has helped us to suggest further questions as well as propose answers to existing problems.

In the next section we develop an ordinary differential equation model which represents *in vitro* studies of LDL oxidation. In Section 3, we discuss enlarging this model to include HDL and some other features present *in vivo* but absent and difficult to reproduce in *in vitro* studies. We present numerical simulations which examine the effects of HDL and antioxidants on the system, showing in particular that HDL can offer protection against oxidation via an alternative mechanism to the commonly proposed reverse cholesterol transport. The hysteresis behaviour that was discovered in the course of our numerical investigation is then studied analytically in Section 4. Finally in Section 5 we discuss our findings in relation to both *in vivo* and *in vitro* experiments and comment on biological implications and future directions for the work.

## 2. MODEL OF LDL OXIDATION *in vitro*

In this section we develop a preliminary model which represents some of the *in vitro* experiments that have been carried out on LDL oxidation. We use this as a starting point since the results of this preliminary model are directly comparable with experimental data. In Section 3, we extend the model to contexts where there are no *in vitro* results. The *in vitro* studies we attempt to replicate involve isolating, from plasma, a fixed concentration of LDL and then exposing it to a radical generator such as AAPH, which releases water soluble peroxy radicals at a constant rate. The concentration of  $\alpha$ -tocopherol (vitamin E) and peroxidized lipid is then monitored over time. The experimental results observe an initial lag in peroxidation followed by a rapid increase in peroxidation products or LOOHs. The termination of the lag phase coincides with complete  $\alpha$ -tocopherol depletion.

Although there are a range of antioxidants involved in preventing lipoprotein oxidation, we focus on vitamin E ( $\alpha$ -tocopherol) and vitamin C (ascorbate), as these have been found to play a pivotal role in determining the point at which lipid peroxidation begins (Frei *et al.*, 1989; Ingold *et al.*, 1993). Thus, the number of unoxidized vitamin E molecules that a lipoprotein possesses is important in determining how long it can survive radical attack. Consequently we divide LDLs into subpopulations according to how many unoxidized vitamin E's the particle possesses. We assume that LDL particles all contain six vitamin E molecules (the average number *in vivo*), and use variables  $L_1(t), \dots, L_6(t)$  and  $L_{ox}(t)$ , where  $L_i(t)$  is the concen-



This model contains three parameters;  $p_r$  depends on experimental protocol, and  $k_e$  can be taken directly from experimental data, as  $3 \mu\text{M}^{-1} \text{s}^{-1}$  (Ingold *et al.*, 1993) (this is for a peroxy radical). For  $k_{e0}$ , experimental results by Ingold *et al.* (1993) give the rate constant for hydrogen abstraction from a bisallylic methylene group of a fatty acid to be  $6 \times 10^{-5} \mu\text{M}^{-1} \text{s}^{-1}$ . As LDL lipoproteins are composed of these groups and this process corresponds to the final stages of lipid oxidation it seems reasonable to use this estimate for our rate constant  $k_{e0}$ .

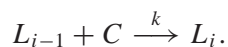
In Fig. 3 we simulate experiments by Neuzil *et al.* (1997) [other examples of this type of experiment can be found in Bowry and Stocker (1993), and Frei *et al.* (1988)] where  $2.0 \mu\text{M}$  of LDL was incubated with  $50.0 \text{ mM}$  of AAPH, which generates peroxy radicals at a rate of between  $1.0 \times 10^{-6}[\text{AAPH}] \text{s}^{-1}$  and  $5.7 \times 10^{-7}[\text{AAPH}] \text{s}^{-1}$  (Ingold *et al.*, 1993). We observe that our model predicts a lag time of 14 minutes, comparable to the experimental results of 18–22 minutes. In the experiments the LDL particles contain additional antioxidants, in particular ubiquinol-10, that are absent from our model. Given that ubiquinol-10 is consumed before  $\alpha$ -tocopherol, this could account for the marginally longer lag phase found *in vitro*. We have also been able to successfully simulate experiments where vitamin C is present (results not shown). So we can conclude that the model offers an appropriate and fairly robust means of studying the behaviour of lipoproteins under oxidative stress.

### 3. EXTENDED MODEL

Having established a quantitatively accurate model of *in vitro* experiments on LDL oxidation, we now consider extending the model to include HDL particles and vitamin C. One of our main focuses in doing this is to investigate the degree of protection that HDL particles can confer on LDLs. HDL particles contain either 1 or 0 vitamin E molecules, so that we have new model variables  $H_1(t)$ , the concentration of HDLs with an unoxidized vitamin E,  $H_0(t)$ , the concentration of HDLs with an oxidized vitamin E, and  $\overline{H}_0(t)$ , the concentration of HDLs containing no vitamin E's, oxidized or unoxidized. As in the preliminary model above, the basic oxidation reaction is  $H_1 + R \xrightarrow{k_v} H_0$ .

HDL particles without the protection of an unoxidized vitamin E are oxidized on contact with a free radical. However, ox-HDL is not of interest clinically: *in vivo*, it does not contribute to foam cell formation, and is free to move out of the intima, in contrast to ox-LDL. Therefore we do not monitor ox-HDL levels in the model solutions.

The other key ingredient in our extended model is vitamin C, which acts synergistically on vitamin E. The antioxidant properties of vitamin C enable oxidized vitamin E's ( $\alpha$ -tocopherol radicals) to be reduced back to  $\alpha$ -tocopherol. Hence, an LDL particle in class  $i - 1$  returns to class  $i$ , as follows:



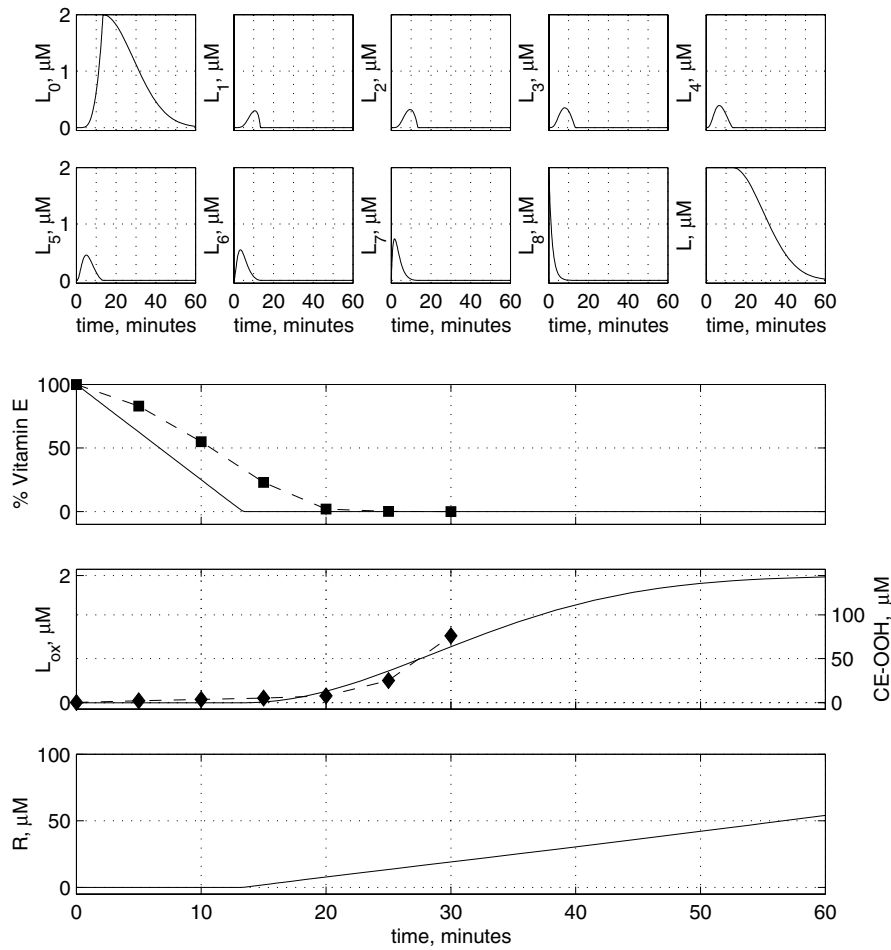


Figure 3. Temporal profile simulating the *in vitro* experiments of Neuzil *et al.* (1997) in which LDL particles are exposed to a constant rate of production of peroxy radicals.  $2 \mu\text{M}$  of gel-filtered healthy human LDL was exposed to  $50 \text{ mM}$  of radical donor under air at  $37^\circ\text{C}$ . At the time points indicated, an aliquot was taken and analysed for  $\alpha$ -TOH and CE-OOH. 100% vitamin E is  $16 \mu\text{M}$  equivalent to eight vitamin Es per particle in our model. The figure includes Neuzil's experimental data for vitamin E percentage (■) and CE-OOH concentration (◆). We plot the model results against the data for vitamin E percentage. The shift between the data and the model is due to the presence of ubiquinol-10 in the experiment. The antioxidant is used before vitamin E thus if it was included in our model we would see a shift in vitamin E consumption to the right. The CE-OOH data is plotted along side  $L_{ox}$  they are both a measure of oxidation, but it is difficult to directly convert between the two. The key observation is the profile shape is the same and most importantly the length of the lag phase is comparable. The oxidant concentration initially remained suppressed while the antioxidants within the LDL particles scavenged the free radical. Once the LDL particles had all reached the  $L_0$  category (a state devoid of vitamin E) lipid peroxidation began. This event corresponds to the end of the lag phase and occurred after 14 minutes, in good agreement with the experimental results. Parameter values and initial conditions used to generate these profiles are as follows:  $k_e = 3 \mu\text{M}^{-1} \text{s}^{-1}$ ,  $k_{e0} = 6 \times 10^{-5} \mu\text{M}^{-1} \text{s}^{-1}$ ,  $p_r = 0.02 \mu\text{M} \text{s}^{-1}$ . Initial conditions are given by  $L_i(0) = 0$ ,  $i = 0, \dots, 5$ ,  $L_6(0) = 2 \mu\text{M}$ ,  $R(0) = 0$ .

Thus in our model an LDL particle in class  $i - 1$  ( $i \geq 2$ ) can either move to class  $i$  by reaction with vitamin C, or to class  $i - 2$  by reaction with a free radical. This is a simplification of the reality, in which movement between LDL classes is a two-stage process with a vitamin E radical as an intermediate [see Stocker (1999), and Upston *et al.* (1999) for a review]. However, the close comparison of the model with *in vitro* data (described above) indicates that this is a good approximation.

We assume a constant vitamin C concentration, which is reflected in the value of the parameter,  $k_c = [C]k$ ; in our model, varying  $k_c$  is equivalent to altering ascorbate levels. A corresponding reaction applies to HDL, with parameter  $k_{ch}$ .

Finally, because we now consider a rather longer timescale than that of minutes in Section 2, we include in the model constant influx rates  $p_h$  and  $p_l$  of HDL and LDL particles, and constant removal rates  $d_h$  and  $d_l$  of unoxidized lipoproteins. As in Section 2, we include a constant rate of free radical production,  $p_r$ , which we vary in order to investigate how much protection HDL can afford LDL, but in addition, we include a background oxidant decay, at rate  $d_r$ .

Thus our extended model equations are

LDL:

$$\begin{aligned} \frac{dL_0}{dt} &= \underbrace{\text{Influx into intima}} + \underbrace{\text{Vitamin E oxidized}}_{k_e R L_1} - \underbrace{\text{Vitamin C donating electron}}_{k_c L_0} - \underbrace{\text{Leaving intima}}_{d_l L_0} - \underbrace{\text{Lipid oxidation}}_{k_{e0} R L_0} \\ \frac{dL_i}{dt} &= + k_e R (L_{i+1} - L_i) + k_c (L_{i-1} - L_i) - d_l L_i \quad (\text{where } i = 1, \dots, 5) \\ \frac{dL_6}{dt} &= p_l - k_e R L_6 + k_c L_5 - d_l L_6 \\ \frac{dL_{ox}}{dt} &= + k_{e0} R L_0 \end{aligned}$$

HDL:

$$\begin{aligned} \frac{dH_0}{dt} &= \underbrace{\text{Influx into intima}} + \underbrace{\text{Vitamin E oxidized}}_{k_v R H_1} - \underbrace{\text{Vitamin C donating electron}}_{k_{ch} H_0} - \underbrace{\text{Leaving intima}}_{d_h H_1} - \underbrace{\text{Lipid oxidation}}_{k_{v0} R H_0} \\ \frac{dH_1}{dt} &= p_{h1} - k_v R H_1 + k_{ch} H_0 - d_h H_1 \\ \frac{dH_0}{dt} &= p_{h0} - d_h H_0 - k_{v0} R H_0 \end{aligned}$$

Free Radical:

$$\frac{dR}{dt} = \underbrace{\text{prod}^n}_{p_r} - \underbrace{\text{Oxidizing Vitamin E}}_{k_e R \sum_{i=1}^6 L_i} - \underbrace{\text{Lipid oxidation}}_{k_{e0} R L_0} - \underbrace{\text{Oxidizing Vitamin E}}_{k_v R H_1} - \underbrace{\text{Lipid oxidation}}_{k_{v0} R (H_0 + \bar{H}_0)} - \underbrace{\text{Other reactions}}_{d_r R} .$$

This is illustrated schematically in Fig. 4.



Table 1. Model parameter values, based on experimental data.

Parameter	Description	Value
$k_e$ ( $k_v$ )	Rate a vitamin E molecule within an LDL (HDL) particle is hit by a free radical.	$3 \mu\text{M}^{-1} \text{s}^{-1}$ ( $0.4 \mu\text{M}^{-1} \text{s}^{-1}$ )
$k_{e0}$ ( $k_{v0}$ )	Rate a lipid particle within an LDL (HDL) particle is hit and oxidized by a free radical.	$6 \times 10^{-5} \mu\text{M}^{-1} \text{s}^{-1}$ ( $7.9 \times 10^{-6} \mu\text{M}^{-1} \text{s}^{-1}$ )
$k_c$ ( $k_{ch}$ )	Rate vitamin C reduces a vitamin E radical back to vitamin E within an LDL (HDL) particle.	$77.5 \text{s}^{-1}$ ( $10.2 \text{s}^{-1}$ )
$d_l$ ( $d_h$ )	Rate LDL (HDL) particles efflux <i>out of</i> the intima and are removed by normal cellular uptake.	$2.4 \times 10^{-5} \text{s}^{-1}$ ( $1.8 \times 10^{-4} \text{s}^{-1}$ )
$d_r$	Radical decay via alternative reactions.	$1.39 \text{s}^{-1}$
$p_l$	Rate of LDL influx <i>into</i> the intima.	$3.84 \times 10^{-5} \mu\text{M} \text{s}^{-1}$
$p_{h0}, p_{h1}$	Influx rate of HDL with 0 and 1 vitamin E respectively.	$1.2 \times 10^{-3} \mu\text{M} \text{s}^{-1}$ , $5.8 \times 10^{-4} \mu\text{M} \text{s}^{-1}$
$p_r$	Rate of free radical production.	Unmeasurable

Note that although this model is closer than that in Section 2 to the actual reactions happening in the intima, it is still a long way from the *in vivo* situation. Key issues missing include the complex and reversible progression of ox-LDL particles, and the possibility of low vitamin C microenvironments due to spatial heterogeneity within the intima. Our equations could potentially form the basis for a (more complex) realistic model of the *in vivo* situation, but our objective here is to study a case which, while it is an extension of current experimental protocols, could potentially be realized *in vitro*.

**Model parameters.** The extended model contains a number of new parameters whose values we now discuss. A summary of all the model parameters is presented in Table 1.

**$\alpha$ , constant of proportionality:**  $k_e, k_{e0}, k_c$  are proportional to  $k_v, k_{v0}, k_{ch}$  as the parameters represent the rate at which LDL and HDL particles are hit, respectively. The constant of proportionality,  $\alpha$  is related to particle size, as this tells us the likelihood of a particle being hit by either a free radical or a vitamin C molecule.

$$\text{ratio, } \alpha = \frac{\text{LDL particle surface area}}{\text{HDL particle surface area}} = \frac{1.02 \times 10^{-3} \mu\text{m}^2}{1.34 \times 10^{-4} \mu\text{m}^2} = \boxed{7.6}.$$

(These measurements are for lipoproteins taken from a typical healthy individual, diabetics for example have smaller particle diameters and there is some size variation within an individual.) Thus an LDL particle is 7.6 times more likely to be hit than an HDL particle is, e.g.,  $k_e = 7.6k_v$  (Bowry *et al.*, 1992).

**$d_l$  and  $d_h$ , LDL and HDL efflux rates:** We take these rates to be based on experimental data from rabbits, where LDL particles take of the order of 8 hours to leave the intima (Schwenke and Carew, 1989; Tozer and Carew, 1997). Thus,  $d_l = \ln 2/8 \text{ h} = 2.4 \times 10^{-5} \text{ s}^{-1}$  and so,  $d_h = 7.6d_l = 1.8 \times 10^{-4} \text{ s}^{-1}$  (HDL particles are smaller so leave the intima at a faster rate.)

**$p_h$  and  $p_l$ , HDL and LDL influx rates:** Again, we base these parameters on estimates of influx rates into the intima *in vivo*. We can estimate the ratio,  $p_h/p_l$ .

- (i)  $p_h$  is 7.6 larger than  $p_l$  due to the size differences between HDL and LDL, resulting in HDL diffusing through the endothelium more rapidly (Bjornheden *et al.*, 1996; Nielsen, 1996).
- (ii)  $p_h$  is also a further six times greater than  $p_l$  because within the blood vessel lumen there are on average six times more HDL molecules than LDL (Geigy Scientific Tables, 0000), hence we would expect the concentration of particles entering into the intima to be effected by this relation.

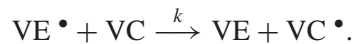
Therefore we have  $p_h = 7.6 \times 6p_l = 45p_l$ , where  $p_h = p_{h0} + p_{h1}$ . Note that experimental evidence reveals that in the blood only 4 in 10 HDL particles contain a vitamin E (Bowry *et al.*, 1992), therefore  $p_{h1} = p_{h0}0.4/0.6 = p_{h0}2/3$ .

In the absence of free radicals, plasma concentrations of lipoproteins are due to a balance between entering and leaving the intima. Thus

$$p_l = d_l[\text{LDL}],$$

$[\text{LDL}] = 1.6 \mu\text{M}$  in plasma, given the value of  $d_l$  from above we obtain  $p_l = 3.84 \times 10^{-5} \mu\text{M s}^{-1}$ . Applying  $p_h = 6 \times 7.6 \times p_l$  yields  $p_{h0} = 1.2 \times 10^{-3} \mu\text{M s}^{-1}$  and  $p_{h1} = 5.8 \times 10^{-4} \mu\text{M s}^{-1}$ .

**$k_c$ , rate of vitamin C reduction of vitamin E:** Packer *et al.* (1979) measured the rate constant for the following reaction:



We assume that if a vitamin C molecule hits an LDL particle containing a  $\alpha$ -tocopherol radical then it would donate one electron at a rate independent of the number of vitamin E's requiring an electron. i.e.,  $[\text{VE} \bullet] \equiv [\text{LDL}]$  ( $[\ ] =$  concentration). As we are assuming the vitamin C concentration is constant, in our model,  $k_c = k[\text{VC}]$ . Data gives  $k = 1.55 \mu\text{M}^{-1} \text{ s}^{-1}$  (Packer *et al.*, 1979). We base our constant vitamin C concentration on *in vivo* plasma levels, which vary between  $20 \mu\text{M}$  (poor diet) and  $200 \mu\text{M}$  (supplemented diet);  $50 \mu\text{M}$  is the average plasma vitamin C concentration of a healthy adult (Jialal *et al.*, 1990), and the corresponding value of  $k_c = 77.5$ ; similarly we can derive the corresponding  $k_{ch}$  for HDL particles.

**$d_r$ , rate of oxidant decay:** We estimate the half life of the free radical to be of the order of 0.5 seconds as oxidants avidly react with a diverse range of molecules. This yields,  $d_r = 1.39 \text{ s}^{-1}$ .

**3.1. Solution of the extended model.** Having established that the key events of *in vitro* lipoprotein oxidation can be captured by our model we study the extended system which attempts to capture some of the additional steps present *in vivo*. We observe that the steady states of our model are not algebraically simple, and require solving a high order polynomial. By finding the solution of

$$\frac{dL_i}{dt} = 0 \quad \text{for } 0 \leq i \leq 6,$$

it is possible to obtain expressions for  $L_i$  in terms of  $R$ . Similarly, solving  $\frac{dH_0}{dt} = \frac{dH_1}{dt} = \frac{d\bar{H}_0}{dt} = 0$  gives,  $H_i(R)$  and  $\bar{H}_0(R)$ . Substituting these into the steady state equation for the free radical yields

$$p_r = k_e R \sum_{i=1}^6 L_i(R) - k_{e0} R L_0(R) - k_v R H_1(R) - k_{v0} R (H_0(R) + \bar{H}_0(R)) - d_r R. \quad (1)$$

The  $L_i(R)$ ,  $H_i(R)$  and  $\bar{H}_0(R)$  in equation (1) are in fact quotient polynomials in  $R$ . Thus, putting the RHS of equation (1) over a common denominator,  $g(R)$ , we obtain  $p_r = f(R)/g(R)$  where  $f(R)$  and  $g(R)$  are polynomials in  $R$ , of order 11 and 10 respectively.

We need to solve the above equation to find the steady states of the system, and this makes stability analysis analytically intractable. Consequently we begin by examining the numerical simulations of the differential equations to help us obtain a better understanding of the model behaviour. A typical temporal evolution of the solution is presented in Fig. 5. We observe different outcomes depending on the initial conditions. In particular, when we take the initial oxidant level to be quite low, we obtain a state of low free radical levels and a lipoprotein concentration near to plasma concentrations. This is analogous to a healthy individual, where only a low background level of oxidized LDL is present. Under initial conditions of elevated free radical concentrations, we observe a high oxidant environment with a severely depleted pool of unoxidized LDL and HDL; ox-LDL concentrations continue to increase, which would be equivalent to a progression to a disease state *in vivo*. We also observed that in low free radical states the distribution of LDLs is heavily skewed towards class  $L_6$ ; conversely, in the high oxidant state (corresponding to disease *in vivo*) the system is skewed towards  $L_0$ . This phenomenon is determined by the ratio of the parameters  $k_c$  and  $k_e R$ . When the radical is well tolerated

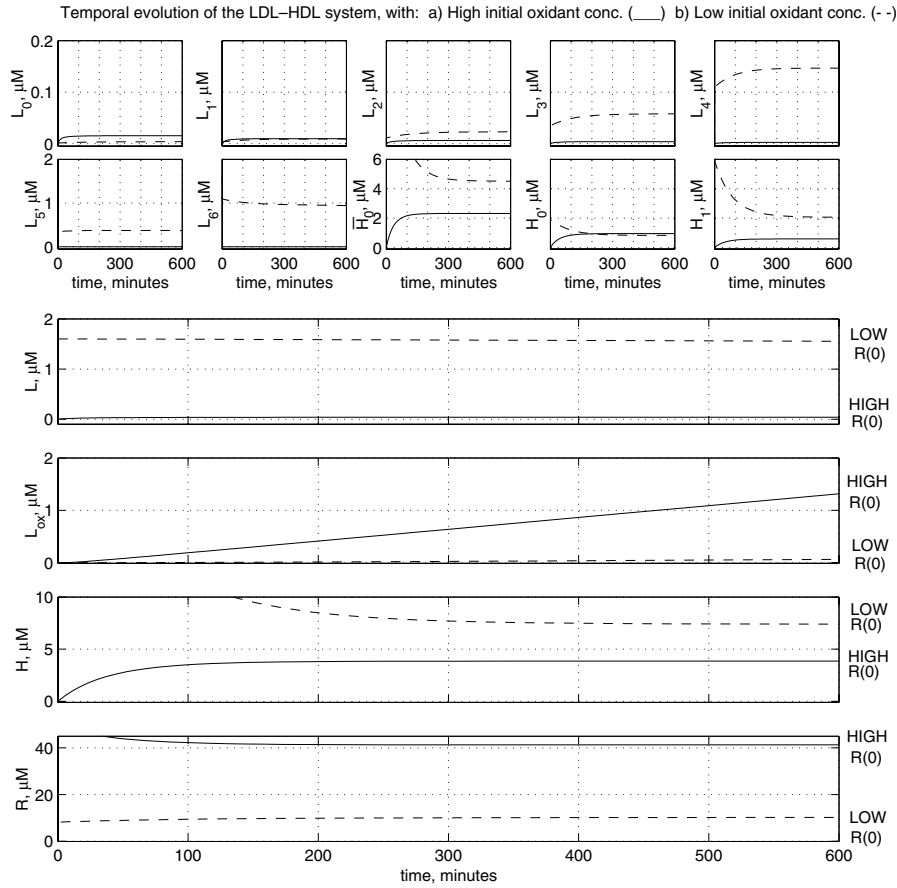


Figure 5. An illustration of a typical numerical simulation of the model, solved using a stiff ODE solver. [The solver used is ODE15s from the MATLAB software package, it applies a multistep variable order method based on numerical differentiation formulas (NDFs).] We present the results of adopting two different initial free radical concentrations and see how they evolve to different equilibriums under the same parameter regime. The solid line arises from a high initial oxidant concentration which persists and leaves a system virtually devoid of unoxidized lipid and with the presence of increasing concentrations of ox-LDL. In contrast the dashed line is initiated with a lower free radical concentration. This remains sufficiently low that the LDL particles are effectively protected by the vitamin C molecules present in the system. Parameter values and initial conditions used to generate these profiles are as follows:  $k_e = 3 \mu\text{M}^{-1} \text{s}^{-1}$ ,  $k_v = 0.4 \mu\text{M}^{-1} \text{s}^{-1}$ ,  $k_c = 77.5 \text{s}^{-1}$ ,  $k_{ch} = k_c/7.6$ ,  $d_l = 2.4 \times 10^{-5} \text{s}^{-1}$ ,  $d_h = 1.8 \times 10^{-4} \text{s}^{-1}$ ,  $d_r = 1.39 \text{s}^{-1}$ ,  $p_{h0} = 1.2 \times 10^{-3} \mu\text{M} \text{s}^{-1}$ ,  $p_{h1} = 5.9 \times 10^{-4} \mu\text{M} \text{s}^{-1}$ ,  $p_l = 3.8 \times 10^{-5} \mu\text{M} \text{s}^{-1}$ ,  $k_{e0} = 6 \times 10^{-5} \mu\text{M}^{-1} \text{s}^{-1}$ ,  $k_{v0} = 7.9 \times 10^{-6} \mu\text{M}^{-1} \text{s}^{-1}$ ,  $p_r = 70 \mu\text{M} \text{s}^{-1}$ . Initial conditions are given by  $L_i(0) = 0$ ,  $i = 0, \dots, 5$ ,  $L_6(0) = 1.6 \mu\text{M}$ ,  $\bar{H}_0(0) = 20/3 \mu\text{M}$ ,  $H_0(0) = 0$ ,  $H_1(0) = 10/3 \mu\text{M}$  and for the dashed line  $R(0) = 10 \mu\text{M}$ , for the solid line,  $R(0) = 5000 \mu\text{M}$ .

$k_c \gg k_e R$ , hence LDLs are regenerated virtually instantaneously. The converse is true for a system overwhelmed by radical.

The sensitivity of the results to initial conditions prompted us to numerically investigate the steady states of the system using the Auto package (Doedel *et al.*, 1991). As free radical concentration is key to determining the model outcome, we use oxidant production rate,  $p_r$ , as the bifurcation parameter. This allows us to construct a bifurcation diagram, displaying the steady states and their stability as illustrated in Fig. 6(b).

The bifurcation diagram displays hysteresis, consequently a small change in  $p_r$  close to a hysteresis point can lead to a significant change in behaviour. This behaviour occurred outside the range of radical production rates,  $p_r$ , which are normally studied *in vitro* and this could propose an interesting *in vitro* experiment. The hysteresis we found explains the observed effects of different initial conditions; as the top branch describes a high oxidant steady state with depleted LDL concentrations and the lower branch depicts a low radical equilibrium or in an *in vivo* setting what may correspond to a healthy state. More specifically we find a system at an initially low radical steady state concentration could, by increasing the rate of radical production,  $p_r$ , jump (at pt. 2) to the upper solution branch. An *in vivo* interpretation would be a healthy individual who undergoes detrimental life style changes such as an increase in dietary cholesterol intake or, beginning smoking, resulting in a switch to a disease state. To recover from this requires significantly more work. Radical production has to be reduced to levels less than originally present in the system before the solution can jump back down to the lower branch at point 1 in the diagrams of Fig. 6.

**3.2. Effects of vitamin C (ascorbate).** Studies have demonstrated that dietary supplementation with vitamin C does not always lead to clinical improvement of atherosclerosis (Nyyssonen *et al.*, 1997; Rimm and Stampfer, 1997). This prompted us to examine the effects of parameters such as  $k_c$  on the location of the hysteresis points. As presented in Fig. 6(a) reduced vitamin C concentrations of 20  $\mu\text{M}$ , a level given *in vivo* by a poor diet (Wen *et al.*, 1996), equivalent to decreasing  $k_c$ , has the effect of moving the hysteresis points to the left. The new location of point 2 results in the solution switching from a low oxidant to a high oxidant profile at a much lower level of radical production,  $p_r$ . Similarly, increasing vitamin C levels, to 200  $\mu\text{M}$ , which can be achieved via dietary supplementation *in vivo*, has the opposite effect and the hysteresis points move to the right. Hence under elevated vitamin C the system can tolerate a much higher rate of oxidant generation before an equilibrium with extensive lipid peroxidation is forced to be established. This observation agrees with an animal model of Panda *et al.* (2000) which investigated the relation between cigarette smoke induced oxidative damage and tissue ascorbate levels.

We can use the bifurcation diagrams to understand the epidemiological results mentioned above. If we begin with typical *in vivo* vitamin C concentrations ( $\sim 50$

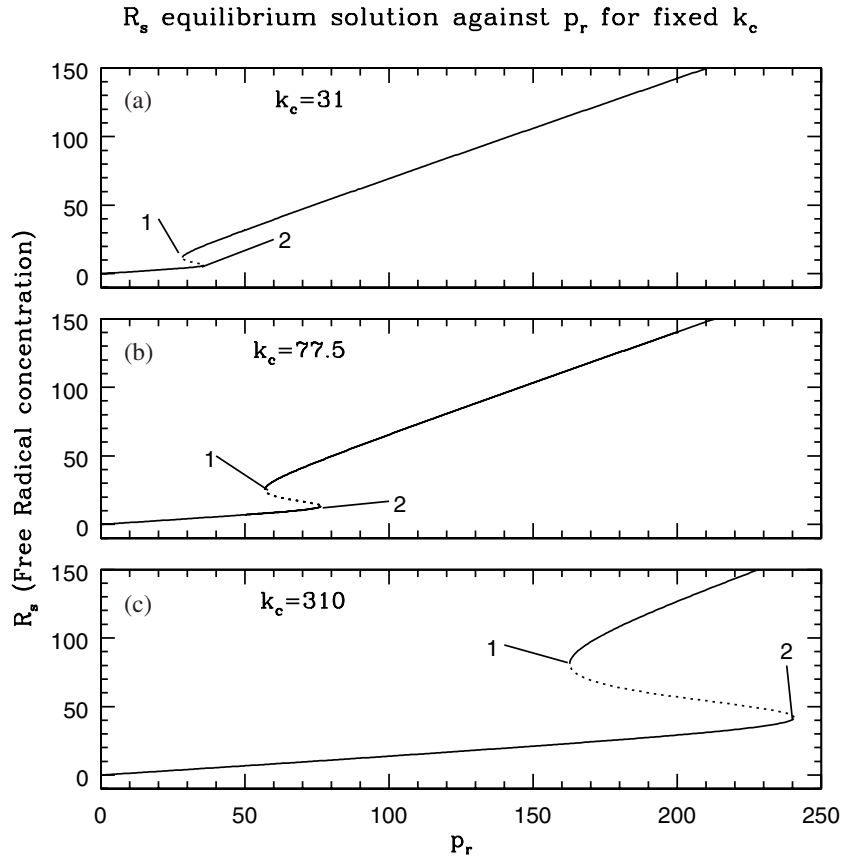


Figure 6. Bifurcation diagrams illustrating the effect of increasing vitamin C concentration. Graph (a) corresponds to a vitamin C concentration of  $20 \mu\text{M}$  ( $k_c = 31 \text{ s}^{-1}$ ), a poor diet *in vivo*. Profile (b) has  $50 \mu\text{M}$  of vitamin C ( $k_c = 77.5 \text{ s}^{-1}$ ), normal levels, and finally graph (c) has a supplementation to a concentration of  $200 \mu\text{M}$  of vitamin C. The graphs show how the equilibrium free radical concentration changes with the parameter  $p_r$ . As  $k_c$  increases points 1 and 2 occur at higher values of  $p_r$  (rate of free radical production). So, for increasing  $k_c$  the window of  $p_r$  values for which the lower solution branch exists widens; this branch can be regarded as a healthy state in an *in vivo* context. Parameter values and initial conditions used to generate these profiles are as follows:  $k_e = 3 \mu\text{M}^{-1} \text{ s}^{-1}$ ,  $k_v = 0.4 \mu\text{M}^{-1} \text{ s}^{-1}$ ,  $k_{ch} = k_c/7.6$ ,  $d_l = 2.4 \times 10^{-5} \text{ s}^{-1}$ ,  $d_h = 1.8 \times 10^{-4} \text{ s}^{-1}$ ,  $d_r = 1.4 \text{ s}^{-1}$ ,  $p_{h0} = 1.2 \times 10^{-3} \mu\text{M} \text{ s}^{-1}$ ,  $p_{h1} = 5.8 \times 10^{-4} \mu\text{M} \text{ s}^{-1}$ ,  $p_l = 3.8 \times 10^{-5} \mu\text{M} \text{ s}^{-1}$ ,  $k_{e0} = 6 \times 10^{-5} \mu\text{M}^{-1} \text{ s}^{-1}$ ,  $k_{v0} = 7.9 \times 10^{-6} \mu\text{M}^{-1} \text{ s}^{-1}$ .  $p_r$  and  $k_c$  vary as displayed on the graphs. Initial conditions are given by  $L_i(0) = 0$ ,  $i = 0, \dots, 5$ ,  $L_6(0) = 1.6 \mu\text{M}$ ,  $\bar{H}_0(0) = 20/3 \mu\text{M}$ ,  $H_0(0) = 0 \mu\text{M}$ ,  $H_1(0) = 10/3 \mu\text{M}$ ,  $R(0) = 1000 \mu\text{M}$ .

$\mu\text{M}$ ), but a high oxidant production rate ( $p_r = 180 \mu\text{M s}^{-1}$ ), equivalent *in vivo* to heavy smoking say, then the equilibrium is situated on the top branch in Fig. 6(b). If we then supplement the system with additional ascorbate to give vitamin C concentrations of  $\sim 200 \mu\text{M}$ , the solution starts on the top branch of Fig. 6(c) and remains there. Hence the extensive lipid peroxidation persists with the vitamin C having only a very limited effect. This phenomenon is a result of most of the LDL particles residing in class 0,  $L_0$ , so that adding vitamin C cannot regenerate the lipoproteins quickly enough to cope with the continual free radical attack. The only way that such a vitamin supplementation would work is if the level of radical production,  $p_r$ , at that time was such that the top branch did not exist in Fig. 6(c) (e.g.,  $150 \mu\text{M s}^{-1}$ ). So on the addition of ascorbate the top branch vanishes and the solution jumps down to the lower branch and what may be regarded as a healthy profile. Investigating this phenomenon experimentally could help understanding of the lack of success of antioxidant supplementation in clinical trials (Nyyssonen *et al.*, 1997).

The effect that the parameter  $k_c$  has on the hysteresis points is of much interest when studying the hysteresis displayed by the system and we use this to mathematically investigate this phenomenon in the next section.

**3.3. Effects of altering plasma HDL concentration.** It is widely recognized that low plasma HDL levels are associated to atherosclerotic disease and epidemiological evidence has shown high HDL concentrations are protective, with HDL levels providing an inverse predictor of risk to vascular disease (Francis, 2000). As the significance of HDL protection is an important question for our model, we also investigated the effect of HDL plasma concentrations on the location of the hysteresis points. We alter the HDL intima influx rate,  $p_h$ . As discussed in the ‘parameter values’ section, this is equivalent to altering the steady state lipoprotein density. Studies indicate that low HDL can be regarded as being less than  $1.25 \mu\text{M}$ , which is about an eighth of normal healthy plasma levels. So we studied the effect of decreasing and increasing plasma HDL by a factor of eight. Qualitatively this has the same effect as altering vitamin C concentration. However, decreasing  $p_h$  also increased the steady state oxidant concentration,  $R_s$  associated with the hysteresis points. Conversely, increasing  $p_h$  decreased  $R_s$ . This directly demonstrates the importance of HDL in preventing LDL oxidation, moreover it suggests that a protective mechanism of absorption of free radical attack may exist rather than protection solely via reverse cholesterol transport.

#### 4. ANALYTICAL INVESTIGATION OF THE HYSTERESIS

The bifurcation diagrams for our system were found to display hysteresis. The location of the hysteresis points on these diagrams is of interest both mathematically and biologically. This prompted us to investigate the behaviour in more detail. A key question about this phenomenon *in vivo* would be what rate of free radical

production,  $p_r$ , leads to a switch from a healthy state to a disease state and vice versa. Given this we focused attention on the oxidant steady state equation. We are able to write down the steady states of our system explicitly, however they are algebraically ‘messy’. The form of the radical steady state equation is

$$p_r = \frac{f(R)}{g(R)}, \quad (2)$$

where  $f$  and  $g$  are polynomials in  $R$ , this is derived in Section 3.1. A plot of this illustrates the turning points of  $f/g$  are our hysteresis points (see Fig. 7). We will focus on obtaining an expression for the first of these points,  $p_r^1$ .  $p_r^2$  has proved much harder to study, and the system cannot be easily simplified in this region of parameter space. Furthermore  $p_r^1$  provides a useful indication of the minimum radical generation rates required to observe the hysteresis phenomenon. To achieve an expression for  $p_r^1$  we revert back to the original ODE equations and make some simplifying assumptions. While retaining as much generality as possible, the philosophy of our argument involves regarding  $k_{v0}$ ,  $d_h$ ,  $k_v$  and the corresponding LDL parameters as fixed. We then consider how  $R$  varies with  $k_c$ . This approach is supported by experimental data which provides strong evidence for fixed numerical values of many parameters, but not  $k_c$ ; furthermore the significance of the parameter  $k_c$  has been demonstrated numerically in Section 3.

**4.1. First hysteresis point,  $p_r^1$ .** To reduce the complexity of the system we first neglect the background decay terms,  $d_l L_i$  and  $d_h H_i$ . These terms are small relative to the remaining terms. For example, if we consider  $\overline{H_0}$ , the exact steady state equation as a function of  $R$  is

$$\overline{H_0} = \frac{p_{h0}}{k_{v0}R + d_h}.$$

For realistic parameter values,  $k_{v0} \sim 10^{-4}$ ,  $d_h \sim 10^{-4}$ , and given that the hysteresis point,  $p_r^1$  occurs for large oxidant concentrations,  $R \sim 10^2$ . This yields

$$\overline{H_0} \approx \frac{p_{h0}}{10^{-2} + 10^{-4}} \approx \frac{p_{h0}}{10^{-2}}.$$

Thus it follows that to leading order,  $\frac{p_{h0}}{k_{v0}R}$  is a good approximation to  $\overline{H_0}$ . A similar argument for the remaining steady state equations implies that to leading order the  $d_l L_i$  and  $d_h H_i$  terms can be neglected. This yields the following simplified steady state equations for the LDL and HDL particles,

$$L_i = \frac{p_l}{k_e R} \left( \sum_{j=0}^{i-1} \left( \frac{k_c}{k_e R} \right)^j + \left( \frac{k_c}{k_e R} \right)^i \frac{k_{e0}}{k_e} \right),$$

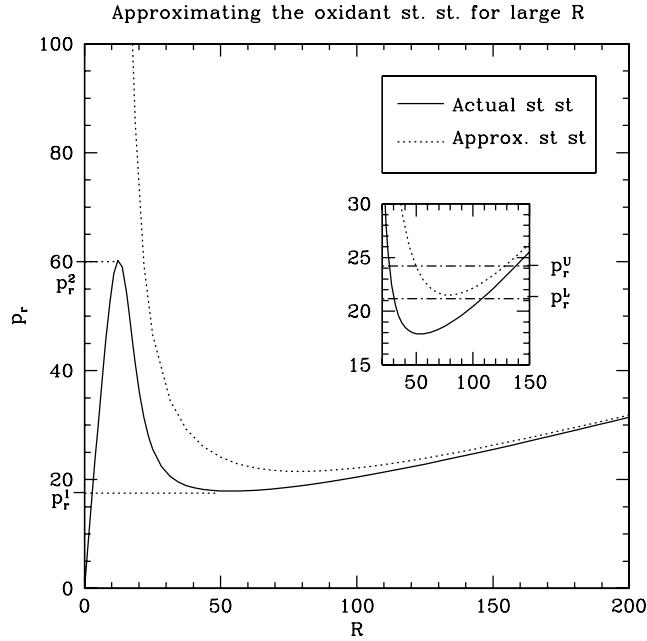


Figure 7. Graph illustrating the free radical steady state associated to different oxidant production rates,  $p_r$ . The solid line (—) is a profile of the exact solution [equation (2)] and the dotted line ( $\cdots$ ) is an approximate solution, [equation (2) where the lipoprotein decay rates,  $d_l$  and  $d_h$  were taken as zero]. The two hysteresis points of the bifurcation diagram are labelled  $p_r^1$  and  $p_r^2$ . The inserted plot shows lower and upper bounds for the approximate solution,  $p_r^L$  and  $p_r^U$  respectively. The approximate solution breaks down for smaller  $R$  and hence the lower bound does not bound the exact solution. Parameter values used to generate these profiles are as follows:  $k_e = 3 \mu\text{M}^{-1} \text{s}^{-1}$ ,  $k_v = 0.4 \mu\text{M}^{-1} \text{s}^{-1}$ ,  $k_c = 77.5 \text{s}^{-1}$ ,  $k_{ch} = k_c/7.6$ ,  $d_l = 2.4 \times 10^{-5} \text{s}^{-1}$ ,  $d_h = 1.8 \times 10^{-4} \text{s}^{-1}$ ,  $d_r = 0.139 \text{s}^{-1}$ ,  $p_{h0} = 1.2 \times 10^{-3} \mu\text{M} \text{s}^{-1}$ ,  $p_{h1} = 5.9 \times 10^{-4} \mu\text{M} \text{s}^{-1}$ ,  $p_l = 3.8 \times 10^{-5} \mu\text{M} \text{s}^{-1}$ ,  $k_{e0} = 6 \times 10^{-5} \mu\text{M}^{-1} \text{s}^{-1}$ ,  $k_{v0} = 7.9 \times 10^{-6} \mu\text{M}^{-1} \text{s}^{-1}$ .  $p_r$  varies as displayed on the graphs.

$$H_0 = \frac{p_{h1}}{k_{v0}R}, \quad H_1 = \frac{p_{h1}}{k_v R} \left( 1 + \frac{k_{ch}}{k_{v0}R} \right), \quad \overline{H_0} = \frac{p_{h1}}{k_{v0}R}.$$

Before substituting these expressions into our steady state equation for  $R$  we make some further observations which allow us to obtain manageable expressions for a lower and upper bound for the hysteresis point,  $p_r^1$ . For the purposes of this calculation it proves useful to non-dimensionalize the free radical variable,  $R$ , to have size 1 in the region of interest. The required scaling is  $R = \frac{p_r}{d_r} R^*$ , where  $R^*$  is our new dimensionless variable. We observed that

$$\frac{k_c}{k_e R} \ll 1 \implies \frac{k_c}{k_e R} \gg \left( \frac{k_c}{k_e R} \right)^i. \quad \text{Moreover,} \quad \frac{k_c}{k_{e0} R} > \frac{k_c}{k_e R} \gg \left( \frac{k_c}{k_e R} \right)^i. \quad (3)$$

Applying our non-dimensionalization yields a condition on our parameters in order that the approximations will hold:

$$\frac{k_c}{k_e R} = \left( \frac{k_c d_r}{k_e p_r} \right) \frac{1}{R^*} \ll 1.$$

Given

$$R^* \approx 1 \text{ we require } \left( \frac{k_c d_r}{k_e p_r} \right) \ll 1.$$

This in fact holds for a wide range of biologically realistic parameter values. This assumption breaks down completely for the second hysteresis point,  $p_r^2$  and consequently simple expressions for the steady states are not so readily obtained.

**Lower bound for  $p_r^1$ .** Using equation (3) it follows that under estimates for the LDL steady states  $L_i$  are given by

$$L_0^L = \frac{pl}{k_{e0}R}, \quad L_1^L = \frac{p_l}{k_e R} \left( 1 + \frac{k_c}{k_{e0}R} \right), \quad L_i^L = \frac{p_l}{k_e R} \left( 1 + \frac{k_c}{k_e R} \right) \quad \text{for } 2 \leq i \leq 6.$$

By substituting this into our steady state equation for  $R$  [equation (1)] we obtain the following:

$$p_r = 7p_l + p_{h0} + 2p_{h1} + \frac{p_l \lambda_0}{R} + \frac{5p_l \lambda}{R} + \frac{p_{h1} \lambda_0}{R} + d_r R \quad (4)$$

where,  $\lambda = k_c/k_e = k_{ch}/k_v$ ,  $\lambda_0 = k_c/k_{e0} = k_{ch}/k_{v0}$  and setting  $p = 7p_l + p_{h0} + 2p_{h1}$ .

If we now solve equation (4) for  $R$  we find

$$R = \frac{p_r - p \pm \sqrt{(p - p_r)^2 - 4d_r p_l \lambda_0 - 4d_r p_l 5\lambda - 4d_r p_{h1} \lambda_0}}{2d_r}. \quad (5)$$

For biologically realistic  $R$ , we require that it is real and non-negative. This is satisfied if

$$p_r \geq p + 2\sqrt{d_r} \sqrt{p_l \lambda_0 + 5p_l \lambda + p_{h1} \lambda_0} = p_r^L. \quad (6)$$

The hysteresis point occurs when  $R$  becomes imaginary. Hence, we find that  $p_r = p_r^L$  is a lower bound for the turning point.

**Upper bound for  $p_r^1$ .** By now over estimating the LDL steady states we can obtain an upper bound for the hysteresis point. A simple form for an upper bound on each  $L_i$  is

$$L_0^U = \frac{p_l}{k_{e0}R}, \quad L_i^U = \frac{p_l}{k_e R} \left( 1 + (i-1) \frac{k_c}{k_e R} + \frac{k_c}{k_{e0}R} \right) \quad \text{for } 1 \leq i \leq 6. \quad (7)$$

As with the lower bound we substitute these estimates for  $L_i$  into the free radical steady state equation, and solve for  $R$ , this yields the following:

$$R = \frac{p_r - p \pm \sqrt{(p - p_r)^2 - 4d_r p_l 6\lambda_0 - 4d_r p_l 15\lambda - 4d_r p_{h1} \lambda_0}}{2d_r}.$$

As before we notice that, when the solution stops existing and becomes imaginary is when the turning point occurs. Thus an upper bound for the turning point is given by

$$p_r = p + 2\sqrt{d_r} \sqrt{\lambda_0 6p_l + \lambda 15p_l + \lambda_0 p_{h1}} = p_r^U.$$

**Modified lower bound.** An illustrative plot of the upper and lower bound is presented in Fig. 7. We observe that  $p_r^L$  is a lower bound for our approximate steady state solution where  $d_l, d_h$  are taken as zero. However, it is not always a lower bound for the exact steady state, as the approximate solution breaks down for smaller  $R$ . This is a consequence of neglecting  $d_h$ , which is an order of magnitude larger than  $d_l$ , so this assumption breaks down first with  $d_h \approx Rk_{v0}$ . We can improve our lower bound by applying  $k_{v0}R \approx d_h$  and noting that we still have,  $k_v R \gg d_h$ . Thus we neglect the  $d_h$  terms in the  $H_1$  steady state equation and for  $H_0$  and  $\overline{H_0}$  we replace  $d_h$  by  $k_{v0}R$ . This yields

$$H_0 = \frac{p_{h1}}{2k_{v0}R}, \quad H_1 = \frac{p_{h1}}{k_v R} \left( 1 + \frac{k_{ch}}{2k_{v0}R} \right), \quad \overline{H_0} = \frac{p_{h1}}{2k_{v0}R}.$$

Note that when  $k_{v0}R \approx d_h$  we have  $k_{e0}R = d_l(7.6)^2 \gg d_l$ , so no modification to the LDL approximation is required. Carrying out the same lower bound calculation as in the ‘lower bound’ section, using the new HDL steady states we obtain

$$p_r = 7p_l + \frac{p_{h0}}{2} + \frac{3p_{h1}}{2} + \frac{p_l \lambda_0}{R} + \frac{5p_l \lambda}{R} + \frac{p_{h1} \lambda_0}{2R} + d_r R.$$

Solving for  $R$  and requiring real and non-negative solutions gives our lower bound  $\widehat{p}_r^L$ :

$$p_r \geq \widehat{p} + 2\sqrt{d_r} \sqrt{\lambda_0 p_l + 5\lambda p_l + \frac{p_{h1} \lambda_0}{2}} = \widehat{p}_r^L,$$

where  $\widehat{p} = 7p_l + \frac{p_{h0}}{2} + \frac{3p_{h1}}{2}$ .

This new lower bound for the modified approximate solution is illustrated in Fig. 8. We notice that  $\widehat{p}_r^L$  is also a lower bound for the exact solution. The accuracy of this bound can be improved further by fine tuning our order of magnitude approximations; however the algebraic form of the bound will remain the same, and this gives the key information regarding what effects the location of this hysteresis point. Furthermore, the free radical concentration  $R$  at which the hysteresis point,  $p_r^1$  occurs increases with vitamin C concentration, so for high values of  $k_c$  the original approximate solution is quite accurate and hence under such conditions,  $p_r^L$  will bound the exact solution as well.

**4.2. Conclusions.** From the lower and upper bound calculations we can see that a key ratio which determines the location of this hysteresis point is  $\lambda = k_c/k_e$ . Increasing the vitamin C concentration increases  $\lambda$  and hence  $p_r^1$ . The magnitude of any benefit provided by vitamin C is explicitly presented in the lower bound expression. Increases in vitamin C allow the system to move from an equilibrium of extensive lipid peroxidation to a state of low oxidant activity, at high radical generation rates, essentially giving the system a greater oxidant tolerance.

Although we have specifically considered LDL particles which have six vitamin E molecules, we can generalize our calculation, for  $n$  vitamin E. This allows us to see the relative effect of vitamin E on the system in comparison to vitamin C.

The general lower bound is given by

$$p_r = \widehat{p}_n + 2\sqrt{d_r} \sqrt{\lambda_0 p_l + \lambda(n-1)p_l + \frac{\lambda_0 p_{h1}}{2}} = \widehat{p}_r^L \quad (8)$$

where  $\widehat{p}_n = (n+1)p_l + \frac{p_{h0}}{2} + \frac{3p_{h1}}{2}$ . Similarly the general expression for the upper bound is as follows:

$$p_r = p_n + 2\sqrt{d_r} \sqrt{\lambda_0 n p_l + \lambda \left( \frac{1}{2}(n+1)^2 - \frac{3}{2}n - \frac{1}{2} \right) p_l + \lambda_0 p_{h1}} = p_r^U \quad (9)$$

where  $p_n = (n+1)p_l + p_{h0} + 2p_{h1}$ .

**Vitamin C vs. vitamin E.** We can compare how the upper and lower bounds vary with vitamin C and vitamin E concentrations to assess the relative effects of the two antioxidants. Specifically this relates to considering the parameters  $k_c$  and  $n$  respectively. In the expressions for  $\widehat{p}_r^L$  and  $p_r^U$  [equations (8) and (9)] we find that the magnitude of the  $p_n$  and  $\widehat{p}_n$  terms are not significantly effected by the number of  $\alpha$ -tocopherol molecules,  $n$ . The relative size of LDL and HDL particles, yields  $p_l \times 6 \times 7.6 = p_h$  as discussed in Section 3. Consequently,  $\widehat{p}_n = (n+1)p_l + \frac{p_{h0}}{2} + \frac{3p_{h1}}{2} \approx \frac{p_{h0}}{2} + \frac{3p_{h1}}{2}$ , at least for values of  $n$  which are biologically realistic we would not expect to find an LDL particle containing much

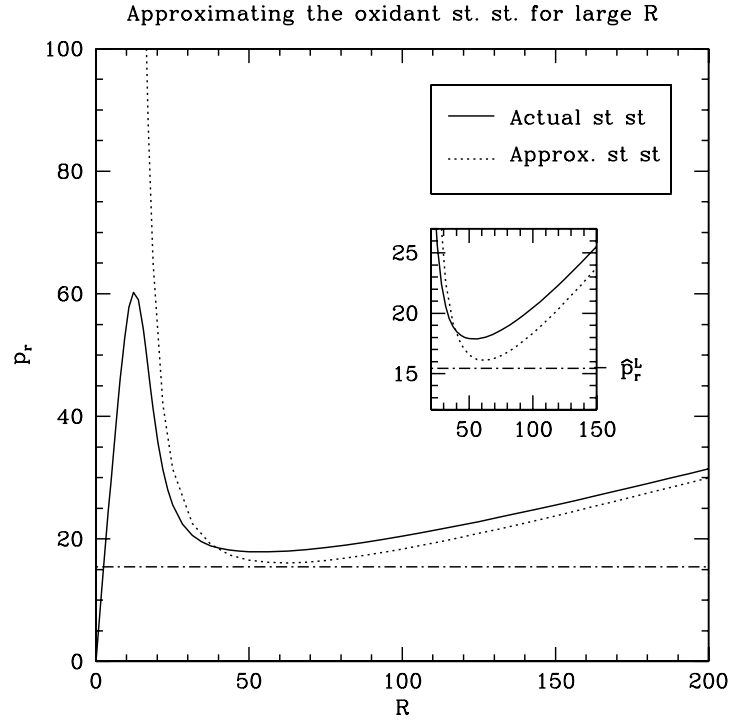


Figure 8. Graph illustrating the free radical steady state associated to different oxidant production rates,  $p_r$ . The solid line (—) is a profile of the exact solution [equation (2)] and the dotted line ( $\cdots$ ) is the modified approximate solution [equation (2) where the LDL decay rate,  $d_l$  was taken as zero and the HDL decay rate,  $d_h \approx Rk_{v0} \ll Rk_e$ ]. The (---) line is a lower bound for the modified approximate solution. This is also a lower bound for the exact solution albeit crude. The inserted plot presents a scaled picture of the hysteresis point  $p_r^1$ . The lower bound is labelled,  $\hat{p}_r^L$ . Parameter values used to generate these profiles are as in Fig. 7,  $p_r$  varies as displayed on the graphs.

more than 15 vitamin E molecules (Esterbauer *et al.*, 1992), solely from the point of view of particle size. A similar argument applies for  $p_n$ . So effects of  $n$  and  $k_c$  on the hysteresis point  $p_r^1$  are confined to the square root terms in our bounds. In both equations (8) and (9) we can factor out a  $\sqrt{k_c}$  term from the square root leaving

$$\hat{p}_n + 2\sqrt{d_r}\sqrt{k_c}\sqrt{\frac{pl}{k_{e0}} + (n-1)\frac{pl}{k_e} + \frac{ph1}{2k_{e0}}} = \hat{p}_r^L \quad (10)$$

$$\text{and } p_n + 2\sqrt{d_r}\sqrt{k_c}\sqrt{\frac{np1}{k_{e0}} + \left(\frac{1}{2}(n+1)^2 - \frac{3}{2}n - \frac{1}{2}\right)\frac{pl}{k_e} + \frac{ph1}{k_{e0}}} = p_r^U. \quad (11)$$

Now, we observe that the rate LDL lipid particles are oxidized  $k_{e0}$ , is several orders of magnitude slower than the rate that vitamin E molecules are oxidized,  $k_e$ . Specifically,  $k_{e0} \approx 10^{-5}$  and  $k_e \approx 1$ . Thus,  $\frac{pl}{k_{e0}} \gg (n-1)\frac{pl}{k_e}$  and more-

over,  $\frac{p_{h1}}{k_{e0}} \gg \frac{np_l}{k_{e0}}$  and so the size of the square root term is also not influenced by  $n$ . However, the fact that we can factor out  $\sqrt{k_c}$  reveals that the upper and lower bounds are scaled by vitamin C concentration, despite being virtually unaffected by the number of vitamin E molecules,  $n$ , that the LDL particles possess. This is illustrated in Fig. 9(a), where the bounds are plotted for a range of biologically realistic parameters. We see as predicted, that varying the number of vitamin E molecules per LDL particle has virtually no effect on  $p_r^1$ , for a given vitamin C concentration. We can offer an intuitive explanation, from the fact that at an equilibrium of high free radical concentration all LDL particles are heavily skewed towards class  $L_0$ .  $p_r^1$  is the radical production rate at below which we can switch to a state which could be regarded as healthy in an *in vivo* context, this is influenced by how quickly an LDL particle can move back down an LDL class relative to the rate of radical attack, thus we would not expect the number of classes to have a significant impact on this. Varying vitamin C within physiological levels, while fixing the number of vitamin E molecules per LDL does however significantly effect the location of the hysteresis point. This implies that vitamin C is a more effective antioxidant than vitamin E, suggesting that vitamin E supplementation will have relatively little effect on this feature of the system.

**With HDL vs. a system devoid of HDL.** We have also examined the effect of HDL on the hysteresis point. We have already discussed the importance of HDL in the  $p_n$  and  $\hat{p}_n$  terms of equations (8) and (9); these arguments also carry to the square root terms. If we consider the lower bound in equation (10) the relative particle size of HDL and LDL give  $p_{h1} = \frac{1}{3} \times 7.6 \times 6 \times p_l$ , implying that  $\frac{p_{h1}}{2k_{e0}} \gg \frac{p_l}{k_{e0}}$ . A similar statement can be made about the upper bound in equation (11). Hence we predict that HDL influx dominates the size of  $p_r^1$ . Moreover, vitamin C concentrations have to be increased significantly to scale  $p_r^1$  enough to compensate for the absence of HDL. We present these conclusions numerically in Fig. 9(c). We fixed the number of vitamin E per LDL particle and then removed HDL from the system to consider how vitamin C effected a system devoid of HDL. If we compare to Fig. 9(b) we find the absence of HDL severely reduces  $p_r^1$  showing that recovery to a low free radical state is more difficult in such an environment. If we also make a comparison to Fig. 9(a) we note that removal of HDL is actually worse for the system than a low vitamin E content. This highlights the key importance of high density lipoproteins outside their role in reverse cholesterol transport.

## 5. DISCUSSION

The events leading to the early stages of atherosclerosis have received much attention in recent years. By understanding this phenomenon we can move a step

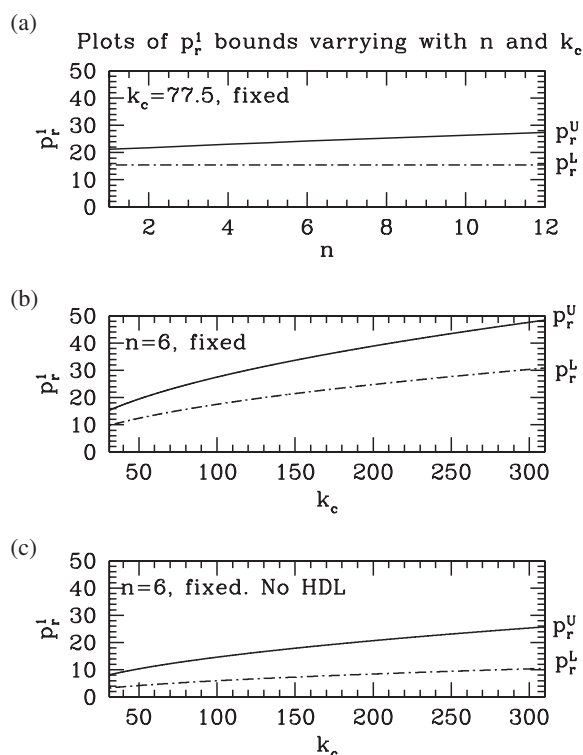


Figure 9. Graph (a) illustrates how the lower and upper bounds for the hysteresis point,  $p_r^l$  vary with the number of vitamin E molecules,  $n$ , per LDL particle, for a fixed vitamin C concentration. The vitamin C concentration was fixed at  $50 \mu\text{M}$ , which is an average level for a healthy individual. Profile (b) shows how the two bounds on  $p_r^l$  vary with vitamin C concentration, reflected by the parameter  $k_c$ . Here  $n$  is fixed at six vitamin E molecules per LDL particle, this is an average number found in plasma LDL. We see that variations in vitamin C concentration have more of an effect than vitamin E. Moreover, for this hysteresis point vitamin E supplementation will not improve a state of high lipid peroxidation as it will not allow an earlier transition to a low radical state under conditions of high levels of oxidant production  $p_r$ . Finally profile (c) illustrates how the bounds on  $p_r^l$  vary with vitamin C concentration in a system devoid of HDL. We see that HDL is very important to the maintenance of a healthy system. Parameter values used to generate these profiles are as detailed in Fig. 7.

closer to establishing a treatment which can arrest further development of the disease. It is widely believed that lipid peroxidation plays a key role in the cholesterol deposition found in the fatty streaks constituting atheroma.

In this paper we investigated the processes involved in lipid oxidation with a view to gaining insight into the mechanisms by which HDL affords protection to LDL. Two models were developed, the first was designed to recreate current *in vitro* experiments. Having achieved this it was then extended to introduce components not present in current experimental protocol, in particular we investigated the interaction between LDL and HDL, in the presence of antioxidants. The system was still

confined to an *in vitro* setting, but the aim was to include additional features present *in vivo*. The mathematical model which we developed gave rise to two principal results. Firstly we found that HDL could provide a protection for LDL against radical attack via an alternative means to the commonly discussed reverse cholesterol transport mechanism. Instead we found that a substantial amount of HDL's protective properties can be found in a much more direct mechanism which can provide a first line of defence. The presence of HDL redirects a substantial amount of oxidant attack away from the more vulnerable LDL particles, thus prolonging the survival time and increasing LDL tolerance to free radical.

The second result concerns the hysteresis behaviour that the system can display. We found that in a range of radical production rates outside those usually studied *in vitro* the model displayed this threshold phenomenon. Once radical production had exceeded a certain level the solution jumped from a low oxidant concentration to high concentrations, *in vivo* this is analogous to a transition from a healthy configuration to a disease state. Recovering from this required significantly more work and the radical production levels had to be reduced to a rate lower than those at which the original jump occurred. Intuition suggests it is not unreasonable to predict such hysteresis.

Current experimental results led us to expect that a high oxidant concentration would be required to overcome the protective properties of vitamin C, motivating the investigation of the effect of higher doses of radical generator. More work is required to examine whether hysteresis is possible within an *in vivo* parameter range, but the possibility is certainly there as the phenomenon can account for the lack of success of late supplementation of vitamin C seen in a recent epidemiological study (Nyyssonen *et al.*, 1997).

Although experimentalists have hypothesised that high radical production may not be appropriate *in vivo* (Ingold *et al.*, 1993), many other factors differ between *in vitro* and *in vivo* work. This includes the binding of lipoprotein to extracellular matrix within the intima. This would expose LDL to high levels of radical attack without the need for a severe increase in radical generation. The timescale of events which occurs over minutes or hours *in vitro*, but over many years *in vivo* leads us to expect the existence or alteration of some pathway within the *in vivo* environment. Despite the likelihood of low radical production rates arising *in vivo*, the many differences between *in vitro* and *in vivo* mean that there may still be qualitatively similar behaviour (e.g., hysteresis), to our model in an *in vivo* environment. It may certainly be worth investigating as it could offer a greater understanding of the system.

Our model also demonstrated the direct beneficial effects of HDL. Moreover our mathematical analysis of Section 4 predicts that the presence of HDL is more beneficial than LDL supplementation with vitamin E. This may explain why the clinical results of the HOPE study (The HOPE Study Investigators, 2000) did not reveal any benefits from increased dietary vitamin E intake. We suggest HDL is protective on two levels, via reverse cholesterol transport and via action as a

sacrificial target for radical attack. Manipulating the way HDL absorbs oxidants is a possibility for future work particularly within the context of a spatial model, where the properties of different subclasses of HDL may become important.

#### ACKNOWLEDGEMENTS

CAC was supported by a studentship from the Engineering and Physical Sciences Research Council. The Centre for Theoretical Modelling in Medicine is supported by a Research Development Grant from the Scottish Higher Education Funding Council.

#### GLOSSARY

**LDL** Low density lipoprotein, a lipoprotein which transports lipid and cholesterol to cells and tissues around the body.

**HDL** High density lipoprotein, a smaller denser form of lipoprotein.

**$\alpha$ -tocopherol** Vitamin E, an antioxidant present within lipoprotein particles.

**Ascorbate** Vitamin C, an aqueous antioxidant which can synergistically work with vitamin E to prevent lipoprotein oxidation.

**Free radical** An extremely reactive molecule which scavenges electrons causing oxidation of the target.

**Lipid peroxide** Oxidized form of the lipid present in lipoproteins. The lipid is oxidized on encounter with a free radical.

**Intima** First layer of the blood vessel wall. Lipoproteins transiently move in and out of this region.

#### REFERENCES

- Bjornheden, T., A. Babiy, G. Bondjers and O. Wiklund (1996). Accumulation of lipoprotein fractions and subfractions in the arterial wall, determined in an in vitro perfusion system. *Atherosclerosis* **123**, 43–56.
- Bonnefont-Rousselot, D., P. Therond, J. Beaudoux, J. Peynet, A. Legrand and J. Delattre (1999). High density lipoproteins (HDL) and the oxidative hypothesis of atherosclerosis. *Clin. Chem. Lab. Med.* **37**, 939–948.
- Bowry, V. W., K. K. Stanley and R. Stocker (1992). High density lipoprotein is the major carrier of lipid hydroperoxides in human blood plasma from fasting donors. *Proc. Natl. Acad. Sci. USA* **89**, 10316–10320.
- Bowry, V. W. and R. Stocker (1993). Tocopherol-mediated peroxidation. The prooxidant effect of vitamin E on the radical-initiated oxidation of human low-density lipoprotein. *J. Am. Chem. Soc.* **115**, 6029–6044.

- Bowry, V. W. and K. U. Ingold (1999). The unexpected role of vitamin E ( $\alpha$ -tocopherol) in the peroxidation of human low-density lipoprotein. *Acc. Chem. Res.* **32**, 27–34.
- Cox, D. A. and M. L. Cohen (1996). Effects of oxidised low-density lipoprotein on vascular contraction and relaxation: clinical and pharmacological implications in atherosclerosis. *Pharmacol. Rev.* **48**, 3–19.
- Davies, M. J. and N. Woolf (1990). *Atherosclerosis in Ischaemic Heart Disease. Volume 1: The Mechanisms*, London: Science Press.
- Doba, T., G. W. Burton and K. U. Ingold (1985). Antioxidant and co-antioxidant activity of vitamin C. The effect of vitamin C, either alone or in the presence of vitamin E or a water-soluble vitamin E analogue, upon the peroxidation of aqueous multilamellar phospholipid liposomes. *Biochim. Biophys. Acta* **835**, 298–303.
- Doedel, E. J., H. B. Keller and J. P. Kernevez (1991). Numerical analysis and control of bifurcation problems: (I) bifurcation in finite dimensions. *Int. J. bifurcation Chaos* **1**, 493–520.
- Esterbauer, H., J. Gebicki, H. Puhl and G. Jurgens (1992). Review Article: The role of lipid peroxidation and antioxidants in oxidative modification of LDL. *Free Radic. Biol. Med.* **13**, 341–390.
- Francis, G. A. (2000). High density lipoprotein oxidation: in vivo susceptibility and potential in vivo consequences. *Biochim. Biophys. Acta* **1483**, 217–235.
- Frei, B., L. England and B. N. Ames (1989). Ascorbate is an outstanding antioxidant in human blood plasma. *Proc. Natl. Acad. Sci. USA* **86**, 6377–6381.
- Frei, B., R. Stocker and B. N. Ames (1988). Antioxidant defences and lipid peroxidation in human blood plasma. *Proc. Natl. Acad. Sci. USA* **85**, 9748–9752.
- Geigy Scientific Tables. 8th edn, Vol. 3, C. Lentner (Ed.), Basle: Ciba-geigy, pp. 115–125.
- Goldstein, J. L., Y. K. Ho, S. K. Basu and M. S. Brown (1977). Binding site on macrophages that mediates uptake and degradation of acetylated low density lipoprotein, producing massive cholesterol deposition. *Natl. Acad. Sci. USA* **76**, 333–337.
- Hamilton, C. A. (1997). Low-density lipoprotein and oxidised low-density lipoprotein: their role in the development of atherosclerosis. *Pharmacol. Ther.* **74**, 55–72.
- Hazel, A. L. and T. J. Pedley (1998). Alteration of mean wall shear stress near an oscillating stagnation point. *J. Biomech. Eng. - Trans. ASME* **120**, 227–237.
- Ingold, K. U., V. W. Bowry, R. Stocker and C. Walling (1993). Autoxidation of lipids and antioxidation by  $\alpha$ -tocopherol and ubiquinol in homogeneous solution and in aqueous dispersions of lipids: unrecognised consequences of lipid particle size as exemplified by oxidation of human low density lipoprotein. *Proc. Natl. Acad. Sci. USA* **90**, 45–49.
- Jialal, I., G. L. Vega and S. M. Grundy (1990). Physiologic levels of ascorbate inhibit the oxidative modification of low density lipoprotein. *Atherosclerosis* **82**, 185–191.
- Keaney, J. F. Jr, D. I. Simon and J. E. Freedman (1999). Vitamin E and vascular homeostasis: implications for atherosclerosis. *FASEB J.* **13**, 965–976.
- Neumann, S. J., S. A. Berceci, E. M. Sevicik, A. M. Lincoff, V. S. Warty, A. M. Brant, I. M. Herman and H. S. Borovetz (1990). Experimental determination and mathematical model of the transient incorporation of cholesterol in the arterial wall. *Bull. Math. Biol.* **52**, 711–732.

- Neuzil, J., S. R. Thomas and R. Stocker (1997). Requirement for, promotion, or inhibition by  $\alpha$ -tocopherol of radical-induced initiation of plasma lipoprotein lipid peroxidation. *Free Radic. Biol. Med.* **22**, 57–71.
- Nielsen, L. B. (1996). Transfer of low density lipoprotein into the arterial wall and risk of atherosclerosis. *Atherosclerosis* **123**, 1–15.
- Nielsen, L. B. (1999). Atherogenicity of lipoprotein(a) and oxidised low density lipoprotein: insight from in vivo studies of arterial wall influx, degradation and efflux. *Atherosclerosis* **143**, 229–243.
- Niki, E., T. Saito, A. Kawakami and Y. Kamiya (1984). Inhibition of oxidation of methyl linoleate in solution by vitamin E. *J. Biol. Chem.* **259**, 4177–4182.
- Nyyssonen, K., H. E. Poulsen, M. Hayn, P. Agerbo, E. Porkkalarataho and J. Kaikkonen *et al.* (1997). Effect of supplementation of smoking men with plain or slow release ascorbic acid on lipoprotein oxidation. *Eur. J. Clin. Nutr.* **51**, 154–163.
- Packer, J. E., T. F. Slater and R. L. Willson (1979). Direct observation of a free radical interaction between vitamin E and vitamin C. *Nature* **278**, 737–738.
- Panda, K., R. Chattopadhyay, D. Chattopadhyay and I. B. Catterjee (2000). Vitamin C prevents cigarette smoke-induced oxidative damage in vivo. *Free Rad. Biol. Med.* **29**, 115–124.
- Parthasarathy, S., J. Barnett and L. G. Fong (1990). High-density lipoprotein inhibits the oxidative modification of low-density lipoprotein. *Biochim. Biophys. Acta* **1044**, 275–283.
- Rimm, E. B. and M. J. Stampfer (1997). The role of antioxidants in preventive cardiology. *Curr. Opin. Cardiol.* **12**, 188–194.
- Saidel, G. M., E. D. Morris and G. M. Chisolm (1987). Transport of macromolecules in arterial wall in vivo: a mathematical model and analytical solutions. *Bull. Math. Biol.* **49**, 153–169.
- Schwenke, D. C. and T. E. Carew (1989). Initiation of atherosclerotic lesions in cholesterol-fed rabbits. II Selective retention of LDL vs. Selective increases in LDL permeability in susceptible sites of arteries. *Arteriosclerosis* **9**, 908–918.
- Stanbro, W. D. (2000a). Modelling the interaction of peroxynitrite with low-density lipoproteins. I Plasma levels of peroxynitrite. *J. Theor. Biol.* **205**, 457–464.
- Stanbro, W. D. (2000b). Modelling the interaction of peroxynitrite with low-density lipoproteins. II Reaction/Diffusion model of peroxynitrite in low-density lipoprotein particles. *J. Theor. Biol.* **205**, 465–471.
- Stanbro, W. D. (2000c). Modelling the interaction of peroxynitrite with low-density lipoproteins. III The role of antioxidants. *J. Theor. Biol.* **205**, 473–482.
- Steinberg, D., S. Parthasarathy, T. E. Carew, J. C. Khoo and J. L. Witztum (1989). Beyond cholesterol: Modifications of low-density lipoprotein than increase its atherogenicity. *New Eng. J. Med.* **320**, 915–924.
- Stocker, R. (1999). The ambivalence of vitamin E in atherogenesis. *Trends Biochem. Sci.* **24**, 219–223.
- Tall, A. R. (1998). An overview of reverse cholesterol transport. *Euro. Heart J.* **19** (Suppl. A), A31–A35.

- Tall, A. R. (1990). Plasma high density lipoproteins: metabolism and relationship to atherogenesis. *J. Clin. Invest.* **86**, 379–384.
- The HOPE Study Investigators. (2000). Vitamin E supplementation and cardiovascular events in high-risk patients. *N. Engl. J. Med.* **342**, 154–160.
- Tozer, E. C. and T. E. Carew (1997). Residence time of low-density lipoprotein in the normal and atherosclerotic rabbit aorta. *Circ. Res.* **80**, 208–218.
- Upston, J. M., A. C. Terentis and R. Stocker (1999). Tocopherol-mediated peroxidation of lipoproteins: implications for vitamin E as a potential antiatherogenic supplement. *FASEB J.* **13**, 977–994.
- Watanabe, A., N. Noguchi, M. Takahashi and E. Niki (1999). Rate constants for hydrogen atom abstraction by  $\alpha$ -tocopherol radical from lipid, hydroperoxide and ascorbic acid. *Chem. Lett.* **7**, 613–614.
- Wen, Y., S. Killalea, P. McGettigan and J. Feely (1996). Lipid peroxidation and antioxidant vitamins C and E in hypertensive patients. *Irish J. Med. Sci.* **165**, 210–212.

*Received 21 May 2001 and accepted 9 September 2001*